14. APPENDICES

APPENDIX A

MATHEMATICAL MODELLING

A1 THERMAL PROPERTIES

A1.1 Thermal Diffusivity

Hardt and Holsinger (1973) have found that despite thermal diffusivities (k/ρc) in theory being independent of compaction pressure, values for compressed and uncompressed powders differ by as much as an order of magnitude which they attribute to the predominance of surface effects. They have also found that the thermal transport properties depend also on the particle size and on the direction of compression (Hardt and Holsinger, 1973).

A1.2 Thermal Conductivity

Parrott and Stuckes (1975:124-126) have made the following generalisations with regards to the thermal conductivity of isotropic oxides:

- Oxides with a lower atomic weight of the cation show a higher thermal conductivity to that of one with a higher atomic weight. This is attributed to the increasing anharmonicity in the lattice vibrations as the atomic weight of the cation becomes increasingly large to that of the oxygen atom.
- The apparent thermal conductivity has been shown to decrease above 300K until about 1000K where it increases due to radiative heat transfer and
- The thermal conductivity for single crystals is higher than that of a polycrystalline substance.
- Small quantities of impurities lower the thermal conductivity, especially around the peak of the thermal conductivity-temperature curve.
- The addition of a second component to form a solid solution greatly decreases the thermal conductivity. The solid solution disturbs the short range order of the lattice and consequently the phonons responsible for heat conduction, with wavelengths of the order of a few interatomic spacings, are effectively scattered by such disturbances.

Cosgrove *et al* (quoted by Parrott and Stuckes, 1975:126) found that the different conditions used in crystal growth affected the thermal conductivity. A decrease was found with decreasing freezing rate and with increasing temperature gradient at the liquid/solid interface. This was attributed to the degree of microsegragation produced in the crystals as the freezing conditions were changed (Parrott & Stuckes, 1975:126-127).

In general the thermal behaviour of the heterogeneous material, unlike that of a solid solution, lies between that of its components and depends on the volume and distribution of each component (Parrott & Stuckes, 1975:128).

For a mixture of 2 components with the materials arranged in parallel slabs, the relationships represented in Figure A-1 hold:

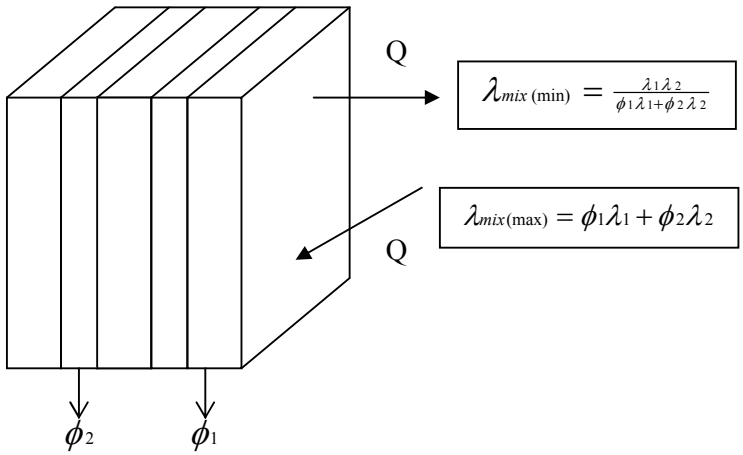

Figure A-1: Simple Parallel-slab Model (Parrott & Stuckes, 1975:130, Godbee and Ziegler, 1966b)

Heat conduction in this arrangement is predominately through the better conductor. However, for heat flow perpendicular to the plane of the slabs the heat flow through each component must be equal but the temperature gradient in each is different as can be seen in Figure A-1. It is dominated by the poorer conductor and is the minimum conductivity of the arrangement (Parrott & Stuckes, 1975:129-130).

Porous Solids

When the thermal conductivity of the fluid is negligible compared to that of the solid, Maxwell's model simplifies to:

$$\frac{\lambda_{mix}}{\lambda_{ccont}} = \frac{1-\phi}{1+\frac{1}{2}\phi}$$

Since the thermal conductivity of air is negligible, porosity levels up to 10-20% merely reduce the observed phonon thermal conductivity. However as the pores are not always spherical, Parrott and Stuckes (1975:133) and Taylor (1986:4921) have found that experimental results can sometimes be fitted rather better to the equation:

$$\lambda_{mix} = \lambda_{cont}(1-\beta_2\phi)$$

A limitation of this expression is that the shape of the pore is not always known. Where the porosity exceeds 25% conduction due to the solid component is reduced by the constriction in the heat flow paths provided by the pores. There are 4 basic heat flow mechanisms that can interact with each other: normal solid conduction, gaseous conduction through the pores, convective heat transfer within the pores and radiation across the pores. Convection can in general be neglected unless the pores exceed about 3mm in diameter; furthermore the contribution due to conduction through the gas is small compared with the solid conductivity (Taylor, 1986:4921-4922). Heat transfer by radiation increases as the pore size increases. As radiation has a T^4 dependence, it plays an increasingly active role at high temperatures. The thermal conductivity will decrease with increasing proportions of glass, liquid and pores although it will start to increase at very high porosities due to the increasing effect of radiative heat transfer (Parrott & Stuckes, 1975:133-134).

Powders

The thermal conductivity of powders is very dependent on the physical texture. For porous samples the low values of thermal conductivity which are obtained are due to the presence of air and also the constriction to heat flow in the solid path at contacts between grains or fibres. Carbon black has a thermal conductivity lower than air due to the presence of a large volume of pores smaller than the mean free path of air molecules. In general, the smaller the particle size, the lower the conductivity. None

of the theoretical models proposed above have good agreement with experimental results as they are too low at room temperature and the experimental conductivities will increase more rapidly with temperature than the model predicts owing to neglect of radiative heat transfer through the air spaces. Lausitz (quoted by Parrott & Stuckes, 1975:145) has commented that although the mathematics is exact, the models used are artificial and radically depart from real powders (Parrott & Stuckes, 1975:144-145).

According to Veale (1972:139) the thermal conductivity of an agglomerated powder in a gas can be calculated by assuming that the heat is transferred by conduction through the solid, by conduction through the gas and by particle to particle radiation. For fine powders, conduction is small owing to the small contact areas between the particles, although these areas may be somewhat increased by the presence of adsorbed layers or preferential condensation of liquid into the saddles between particles. Conductivity is independent of gas pressure as long as the mean free path of the gas molecule is less than the interparticle spacing (Veale, 1972:139-140).

Beck (1984) has used the models proposed by Maxwell and Rayleigh, Russel, Webb, Gorring and Churchill and Kunii and Smith to predict the thermal conductivity of $Sb/KMnO_4$ (quoted in Beck, 1984). He found that the model of Kunii and Smith gave reasonable results.

A2. EXTRACTION OF KINETIC PARAMETERS AND COMBUSTION MODELLING

A number of authors have attempted to mathematically model the combustion wave with mixed success. The earliest theory was based on the Mallard-Le Chatelier theory of propagation, i.e. $v = \frac{\lambda Q}{bc^2 \rho (T_f - T_a)}$ (Quoted by Beck, 1984).

Snegirev and Talalov (1991) have outlined a procedure for recovering kinetic parameters from data of firing a pyrotechnic mixture by an incandescent surface at a constant temperature. They have stated, however, that the combustion time can not be calculated using the kinetic parameters which they derived for the Si-Pb_3O_4 composition as they have not considered the increase in retarding effect of a SiO_2 layer on the Si particles, kinetics of the Pb_3O_4 decomposition and the transport oxidising agent to the zone of combustible material oxidation.

A2.1 Leeds Method for Gasless Pyrotechnic Reactions

Boddington *et al* (1982, 1986) have derived a model for the analysis of temperature profiles for gasless pyrotechnics to obtain information regarding the adiabatic temperature rise and the local instantaneous rate of heat evolution. The model is one of a long cylinder of gasless pyrotechnic mixture, initially and finally at ambient temperature Ta. They have assumed that the temperature excess U=T-Ta over a cross section normal to the axis of propagation is given by:

$$t^* U_{tt} - U_t + G - U t_{th}^{-1} = 0$$

The time $t^* = \lambda / \rho c v^2$ is the rise time of the inert forewave of the profile in the absence of lateral heat transfer. $t_{th} = \rho c / h$ is the thermal relaxation time of the system due to lateral heat transfer. $G = w / c$ is a measure of the local thermal power arising from the heat effects of all the chemical and phase changes. The model is based on the

assumption that the density, thermal conductivity, specific heat capacity etc. are independent of temperature. This model has been further developed by Boddington *et al* (1989, 1990) to allow for a more complex rate law to describe the reaction kinetics at low temperatures and where the global approach used previously predicted too great a reaction rate and to allow for heat loss. The approach is to combine a high temperature diffusion term with an Arrhenius temperature dependence that determines the behaviour at lower temperatures. A limitation of the model is that it makes no allowance for phase changes and is pseudo-one-dimensional (Boddington *et al*, 1989 and 1990).

Drennan and Brown (1992b), Rugunanan and Brown (1994a,b,c), Rugunanan (1991) Beck (1984) have used this method for the extraction of kinetic parameters for binary and ternary mixtures.

A2.2 Combustion Synthesis Reaction Modelling

Munir (1988) has proposed the following equation to calculate the velocity of the combustion front for SHS reactions:

$$v^2 = f(n)\frac{cd}{Q}\frac{RT_c^{\,2}}{E}K_o \exp\left(\frac{-E}{RT}\right)$$

where f(n) is a function of the kinetic order n and T the absolute temperature.

The equation was derived with the following assumptions:

- The thermophysical properties of the product are not strong functions of temperature.
- Convective and radiative heat losses are negligible.
- The width of the reaction zone is narrow in comparison with the thermally affected zone (Munir, 1988).

Varma *et al* (1998) on the other hand have proposed the following equations for the combustion wave velocity in gasless systems:

- For a zero order reaction:

$$v^2 = \frac{2\lambda}{\rho Q}\frac{RT_c^{\,2}}{E}K_o \exp\left(-\frac{E}{RT_c}\right)$$

- For n'th order type kinetics, Varma *et al* (1998) have proposed:

$$v^2 = \frac{(2-n)\lambda}{\rho Q}\frac{RT_c^{\,2}}{E}K_o \exp\left(-\frac{E}{RT_c}\right)$$

This equation is not valid for $n \geq 2$, since it leads to zero (n=2) and imaginary values of velocity for n>2). The origin of this discrepancy is that when the dependence of reaction rate on conversion is sufficiently strong (e.g. for higher order reactions), the reaction rate away from the adiabatic combustion temperature may also be significant. Khaikan and Merzahanov (quoted by Varma *et al*, 1998) derived the following equation for n'th order kinetics:

$$v^2 = \left\{2\left[\Gamma\left(\frac{n}{2}+1\right)\right]^{1-\frac{n}{2}}\left(\frac{n}{2e}\right)^{\frac{n^2}{4}}\right\}\frac{\lambda}{\rho Q}\frac{RT_c^{\,2}}{E}K_o \exp\left(-\frac{E}{RT_c}\right)$$

where $\Gamma(z) = \int_0^\infty e^{-t}t^{z-1}dt$ is the gamma function.

These equations were based on the following assumptions:

- The Lewis number is very small i.e. $Le = \frac{D}{\alpha} <<< 1$. This means that heat conduction occurs much faster than mass diffusion and therefore mass diffusion at a macroscopic scale may be neglected and an average concentration of the reactants in any local region may be used. Density, thermal conductivity and heat capacity are an average of the reactant and product values.
- The temperature and concentration profiles do not change with time (constant pattern propagation).
- There is no heat loss.
- There is one chemical reaction.
- The rate of heat evolution is neglected everywhere except in the narrow zone near T_c (narrow zone approximation) (Varma *et al*, 1998).

This theory applies mainly to kinetic-controlled reactions, but reactions involve many processes. Merzanhov (quoted by Varma *et al*, 1998) compared experimental data with combustion equations for various types of heat sources and concluded that the combustion wave velocity can be represented as follows:

$$v^2 = A(\eta^*, T^*)\exp\left(-\frac{E}{RT^*}\right)$$

Where T^* and η^* are the values of temperature and corresponding conversion which control the combustion front propagation and $A(T^*,\eta^*)$ is a function weaker than the exponential. Merzhanov (quoted by Varma *et al*, 1998) identified 4 types of combustion:

- Combustion with a thin reaction zone (Figure A-2). $\eta^*=1$, $T^* = T_c \approx T_o + \frac{Q}{c}$

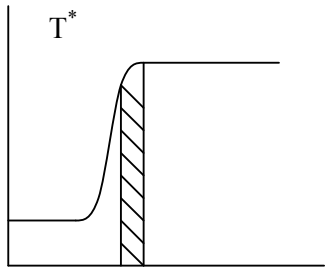

Figure A-2: Temperature Profile for Combustion with a Thin Reaction Zone (Varma et al, 1998)

- Combustion with a wide zone which occurs when a product layer strongly inhibits the reaction (Figure A-3). $T^* = T_o + \frac{Q}{c}\eta^*$, where η^* is determined from:

$$\frac{Q}{c}\frac{\partial\phi(\eta^*,T^*)}{\partial T} + \frac{\partial\phi(\eta^*,T^*)}{\partial\eta} = 0$$

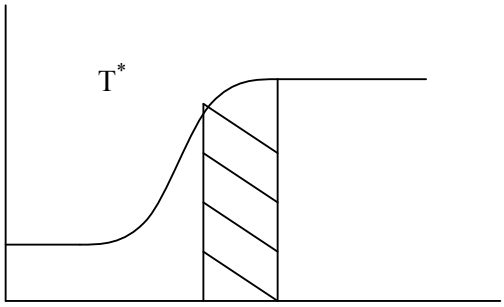

Figure A-3: Temperature Profile for Combustion with a Wide Reaction Zone (Varma et al, 1998)

- Combustion with phase transformations (Figure A-4). $T^*=T_m$ (melting point) and $\eta^* = \frac{(T_m - T_o)}{\left(Q/c\right)}$.

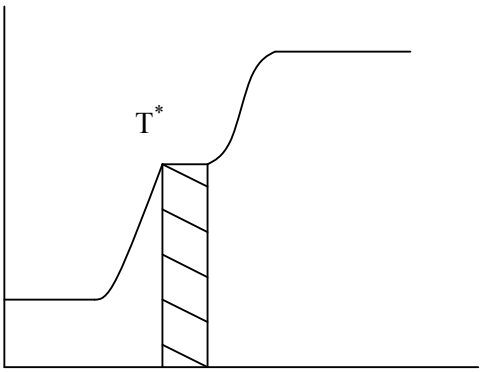

Figure A-4: Temperature Profile for Combustion with Phase Transformations (Varma et al, 1998)

- Combustion with multistage spatially separated reactions (Figure A-5). $\eta^*_1 = 1$ and $T^* \approx T_o + \left(\frac{Q_1}{c}\right)$ where the subscript refers to the first low temperature stage of the complex reaction (Varma *et al*, 1998).

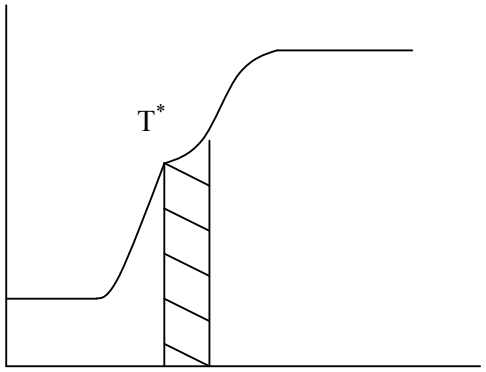

Figure A-5: Temperature Profile for Combustion with Multistage Spatially Separated Reactions (Varma et al, 1998)

Varma *et al* (1998) have further proposed that the temperature profile in the preheating zone be described by:

$T = T_o + (T_c - T_o)\exp\left(\frac{v}{\alpha}x\right)$ where $x \le 0$ and $x_T = \frac{\alpha}{v}$ denotes the characteristic length scale of the combustion wave. The temperature profile in the reaction zone is equal to the combustion temperature.

A2.2.1 Mictrostructural Models

Microstructural models have been developed to account for reactant particle size and distribution, product layer thickness etc and correlate them with the combustion temperature and velocity. The equations used are similar to those in the previous section. However the kinetics of heat release may be controlled by phenomena such as diffusion through a product layer of melting or spreading of reactants. These phenomena often have Arrenhius-type dependencies. The dependence of velocity on particle size has been described as: $v = f(d)F(T)$ (Varma *et al*, 1998)

Four reaction cell geometries have been used in the theoretical models (Varma *et al*, 1998). These include:

1. Alternating lamellae of the two reactants (A and B) which diffuse through a product layer (C) to react i.e. A(s) + B(s) → C(s) (Figure A-6).

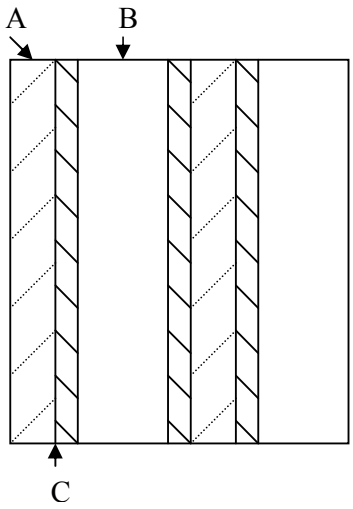

Figure A-6: Reaction Cell Geometry for A(s) + B(s) → C(s) (Varma et al, 1998).

By assuming that the particles are flat, it is possible to neglect the change in the reaction surface area. The characteristic particle size is equivalent to the layer thickness and the relative thickness of the initial reactant layers are determined by stoichiometry. Hardt and Phung (1973) found that $f(d) \propto \frac{1}{d}$

i.e. $v = \frac{0.8\lambda Q}{w_1 a_o \rho c^2 (0.035E - T_o)}$ (all units are British).

Aldushin *et al* (quoted by Varma *et al*, 1998) developed the following kinetic function:

$\phi(\eta, T) = K_o \exp\left(-\frac{E}{RT}\right) e^{-m\eta} \eta^{-n}$ which describes linear (m=0, n=0), parabolic (m=0, n=1), cubic (m=0, n=2) and exponential (m>0, n=0) kinetic dependencies. Combination of these dependencies with the velocity equation yields the following:

i) Power law kinetics (i.e. m=0, n≥0)

$$v = \frac{(n+1)(n+2)}{d^{n+0.5}} F(T)$$

ii) Exponential kinetics (i.e. m>0, n=0)

$$v = \frac{m^2}{(e^m - 1 - m)d} F(T)$$

For a unimodal particle size distribution with particle size distribution function, $\chi(d)$ the effective diameter can be calculation using $d_{eff} = \left[\int_{d_{\min}}^{d_{\max}} d^2 \chi(d) dd\right]^{0.5}$ and used in the above expressions in place of d. For a bimodal distribution, the combustion wave has a two stage structure similar to Figure A1-5, where two combustion fronts propagate in sequence. Using effective particle sizes for fine (d_1) and coarse (d_2) particles the velocity dependence for the leading combustion front is described by:

$U = \frac{F(T)}{\left[d_1^2 m_1 + d_2^2 (1 - m_1)\right]^{0.5}}$ where m_1 is the mass fraction of finer particles (Varma *et al*, 1998).

2. A spherical particle of one reactant (B) is surrounded by a melt of the other reactant (A) and a solid product layer (C) grows on the surface of the particle with the molten reactant diffusing through the product layer i.e. A(l)+B(s)→C(s) (Figure A-7). At a given temperature the concentrations at the interphase boundaries are determined from the phase diagrams of the system (Varma *et al*, 1998).

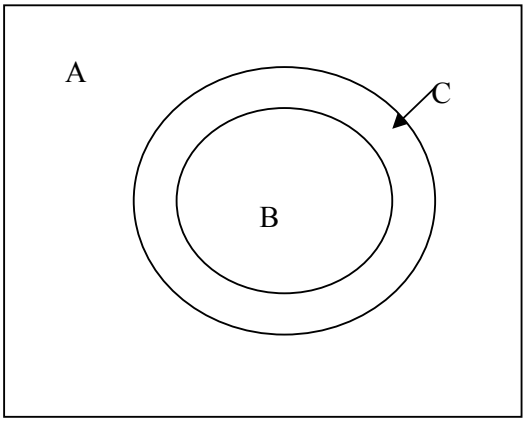

Figure A-7: Reaction Cell Geometry for A(l) + B(s) → C(s) (Varma et al, 1998)

3. Similar to the second cell geometry except that the solid reactant diffuses through an initial product layer to the melt and a liquid product is formed which crystallises in the in the volume of the melt after saturation i.e. A(l)+B(s)→C(l) (Figure A-8). The initial product layer's thickness is assumed to remain constant. Cao and Varma (quoted by Varma *et al*, 1998) reported the combustion wave velocity as being $U = \left[\frac{1}{d}\left(\frac{2}{d}+\frac{1}{\delta}\right)\right]^{0.5} F(T)$ where δ is the thickness of the initial product layer.

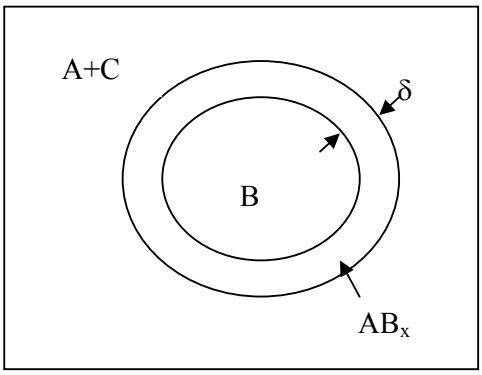

Figure A-8: Reaction Cell Geometry for A(l) + B(s) → C(l) (Varma et al, 1998)

4. Both reactants melt and the liquid product forms in the reaction zone i.e. A(l)+B(l)→C(l) (Varma *et al*, 1998) (Figure A-9). After both reactants melt, their interdiffusion and the formations of a liquid product occur simultaneously. In the kinetic-limiting case, for a stoichiometric mixture of reactants (A and B) the propagation velocity does not depend on the initial reactant particle sizes. For diffusion-controlled reactions the velocity is $v = \frac{b_1}{d} F(T)$ where

$$b_1 = \begin{cases} 1 & \text{if } d < d_B^{st} \\ \dfrac{d^3}{D_{rc}^3 - d^3}\dfrac{v_B MW_B}{v_A MW_A} & \text{if } d > d_B^{st} \end{cases}$$

d_B^{st} is the diameter of reactant B in a corresponding stoichiometric mixture and D_{rc} is diameter of the reaction cell.

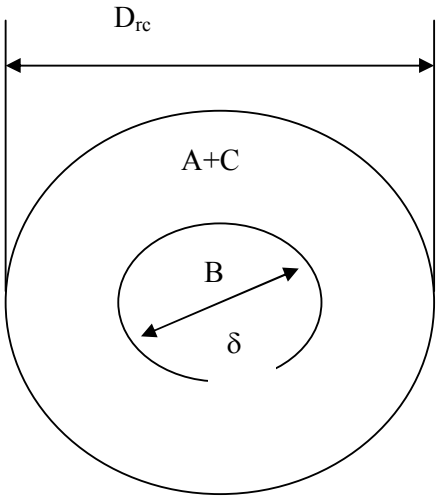

Figure A-9: Reaction Cell Geometry for A(l) + B(l) → C(l) (Varma et al, 1998)

2.2.2 Cellular Models

For cellular models, the reaction medium is divided into a discrete matrix of cells, where the temperature and effective properties are assumed to be uniform throughout the cell. The difference between cellular models and finite difference/element models is that the latter are finite approximations of continuous equations with the implicit assumption that the width of the reaction zone is larger than other length scales (diffusion, heterogeneity of medium etc.). Cellular models have no such assumptions and the local transport processes in a heterogeneous medium is accounted for. Varma *et al* (1998) provide a description of the cellular models which have been reported in literature.

A2.3 Combustion with Gaseous Reaction Products

Varma *et al* (1998) describe the various models which have been derived for filtration combustion, i.e. gas-solid reactions. These models will not be discussed here as they involve the addition of a gaseous reactant which is not the case for pyrotechnic delay reactions, where both reactants are initially solids. However, the model proposed by

Aldushin and Zeinenko (1992) will be discussed to gain an insight into the effect of a gas on the burn characteristics.

It has been shown by Aldushin and Seplyarskii (quoted by Aldushin and Zeinenko, 1992) that the flow of a heat carrier through the reacting medium, in the direction of propagation of the combustion zone, increased the temperature of the zone above the thermodynamic adiabatic combustion temperature. The gas, passing through the reacting mixture, acts as a heat transfer medium, and heats the initial mixture. One characteristic of this system is the inverse relation between the density of the gas flow and the velocity of the reaction wave. In such a system, a state of steady combustion is possible only with spontaneous balancing of the gas separation processes and the effects of the gas flow on the temperature and velocity of propagation of the reaction zone (Aldushin and Zeinenko, 1992).

Based on an isotropic porous pyrotechnic mixture as reacting medium, Aldushin and Zeinenko (1992) have proposed the following equations for the steady combustion front:

$$mc\left(1-\frac{\eta_1 v_1 c_1}{c}\right)T_s' = Qy + \lambda T_s'' + \alpha_2\left(T_g - T_s\right)$$

$$mv_1 c_1(\xi - \eta_1)T_g' = v_1 c_1 y\left(T_g - T_s\right) + \alpha_2\left(T_g - T_s\right)$$

where $m\eta_1 = y$ and $y = K_o \exp\left(-E/RT_s\right) f(\eta_1)$

when $x = -\infty$: $T_s=T_g=T_o$, $\eta_1=0$ and

when $x = \infty$: $T_s=T_g=T_r$, $\eta_1=1$

The above equations are the material and heat balances for the steady combustion wave, counted from right to left, with respect to the spatial variable x and not with the moving reaction front. The terms with dashes are the differentials with respect to x. The parameter, ξ, determines the direction of the gas flow. Depending on the conditions of combustion, the gas can flow in the direction of the moving front ($\xi=1$), or in the reverse direction ($\xi=0$). Aldushin and Zeinenko (1992) have described the detailed derivation of these equations.

Their model is based on the following assumptions:

- The thermophysical properties and the heat of reaction were constant.
- The thermal conductivity of the gas, drop in pressure in the porous layer and heat loss to the surrounding medium were negligibly small.
- Phase transformations did not occur.
- There was no flow of the condensed components.
- The combination of the actual chemical reactions occurring was equivalent to a single overall reaction described by $y = K_o \exp\left(-E/RT_s\right) f(\eta_1)$.
- The boundary conditions were defined by the thermal equilibrium of the phases at large distances from the reaction zone ($x=0$).

From these equations Aldushin and Zeinenko (1992) have derived the following equations:

- The combustion front temperature, T_g:

$$T_g = T_o + \frac{Q}{c_1}\left(1 - \frac{\xi \nu_1 c_2}{c_1}\right)$$

- The combustion mass velocity:

$$m^2 = \frac{\frac{K_o \lambda}{Q}\frac{RT_g^{\,2}}{E}\exp\left(-\frac{E}{RT_g}\right)}{\int_0^1 \frac{(1-\eta_1)d\eta_1}{f(\eta_1)}}$$

According to Aldushin and Zeinenko (1992) the assumption of a narrow chemical reaction zone is consistent with the heat conduction mechanism of combustion wave propagation. During the flow of a gas through the combustion products, this is the only mechanism, whereas when the gas moves with the front, propagation of the reaction can be a convective mechanism, in addition to conduction (Aldushin & Zeinenko, 1992).

Experimentally, Aldushin and Zeinenko (1992) attempted to confirm the possibility of propagation of a steady combustion wave in a porous partially gasified medium and to determine the effect of heat transfer between the gaseous reaction products and the initial material. They used oxygen-containing mixtures based on sodium chlorate

granules. They found that when the flow of the generated oxygen was in the direction of the moving front, the maximum temperature exceeded the combustion front temperature of the products, without taking into account the heat transfer from the gaseous reaction products, but did not exceed the theoretical combustion temperature because of heat losses and the low mass velocity of steady combustion. Furthermore they found that mixtures that burned at a stable constant rate when $\xi=0$ burned at a progressively increasing rate when $\xi=1$. Also, a change in the direction of low for mixtures which were not capable of stable propagation under normal conditions, led to the stabilisation of the combustion. This leads to the assumption that for highly concentrated fuel or compositions of low activity, the change in the direction of gas flow causes the heat transfer mechanism to change. They thus confirmed using the above model experimentally that a steady combustion wave can exist in a porous reacting media composed of chemical sources of pure gases when the gaseous reaction products heat the original material. In this study they have found that the temperature of combustion increases with increasing mass fraction and heat capacity of the released gas and exceeds the adiabatic combustion temperature of the material (Aldushin & Zeinenko, 1992).

Nosgrove *et al* (1991) proposed a model to study the effects of gas production on pyrotechnic compositions. Their model is based on the following assumptions:

- The flow is one-dimensional so that all the variables depend only x the distance down the delay element and on t, the time. This assumption is poor as it neglects heat losses into the detonator wall which is not one-dimensional.
- The temperature of the reacting solid is the same as that of the gas.
- The gas which is released flows under the action of the local pressure gradient according to Darcy's law, but the reacted solid does not move. This implies that permeability is uniform throughout the element length, but the permeability is sensitive to the structure and void fraction of the porous medium which changes as the reaction proceeds.
- Transfer of heat by radiation between the fuel particles may be neglected.
- The gas is an ideal gas.

The resultant equations are:

- Flame Temperature:

$$Tf(\iota) = To + \frac{Q(\rho_0 - \rho_\infty)}{\rho_\infty c_s + (1-\iota)(\rho_0 - \rho_\infty)c_1}$$

- Flame Speed:

$$v^2(\iota) = \frac{\lambda\rho_0(2-l)RT_f{}^2 r(T_f)}{E(\rho_0 - \rho_\infty)^2\left[Q + (c_s - c_1)(T_f - T_0)\right]}$$

They found that the boundary conditions which change as a result of the gas flow can only be used generally to obtain an explicit model and therefore do not describe the effect of the solid to gas conversion and gas flow. They have attempted to solve the problem numerically and found that the direction in which the gas flows and where the detonator is punctured does have an effect on the reaction (Nosgrove et al, 1991).

There has been mixed success for comparing experimental results with these and other theoretical models. The use of simplifying assumptions such as the narrow zone, and one step reaction pose problems. The simplifying assumptions need to be satisfied under experimental conditions in order to obtain intrinsic kinetic data.

A3 TIME TO IGNITION

Boddington *et al* (1986) have measured the times-to-ignition using a temperature-jump technique in order to derive the chemical activation energies. The aim was to raise the temperature of the reagents as quickly as possible from its initial temperature to a temperature, T_a, above the critical temperature. They found that the measurements were not sufficiently precise to discriminate between the various methods which have been proposed by previous authors (quoted by Boddington *et al*, 1986).

A4 COMPUTER MODELLING

Taylor (1994) attempted to use computer modelling to complement the existing experimental techniques used to analyse pyrotechnic compositions. A detailed discussion of his work will not be discussed here.

In summation, Taylor (1994) found the following:

- The one-dimensional model used a simple model (Heat loss through the sides of the column is negligible, heat loss through ends is described by Biot number) and of the column with temperature being calculated at each node at each time step using an explicit method. The method depended on the availability of good kinetic data. It would be beneficial to implement for quick evaluation of compositions.
- The two-dimensional model allows for heat loss and stipulating surrounding material. It had the added advantage of being able to obtain fringe and contour plots and temperature gradients. The model was limited by the quality of the available kinetic data and available computation time.
- The particle-packing model was based on the assumption that the fuel and oxidant particles both had uniform but different radii and that all the particles were spherical.
- The Monte Carlo method incorporated the effect of random packing of the particles on the burn speed.

He recommended that future models allow for the introduction of temperature dependence of properties such as heat capacity etc., non-homogeneous material in the composition (additives), direct incorporation of variables such as compaction and composition and improvement in the models used for kinetic analysis of experimental temperature profiles (Taylor, 1994).

APPENDIX B

EFFECT OF VARYING DATA FILTRATION PARAMETER

APPENDIX C

CALCULATION OF THERMOCHEMICAL REACTION PROPERTIES

APPENDIX D

XRD AND XRF ANALYSIS OF CUO

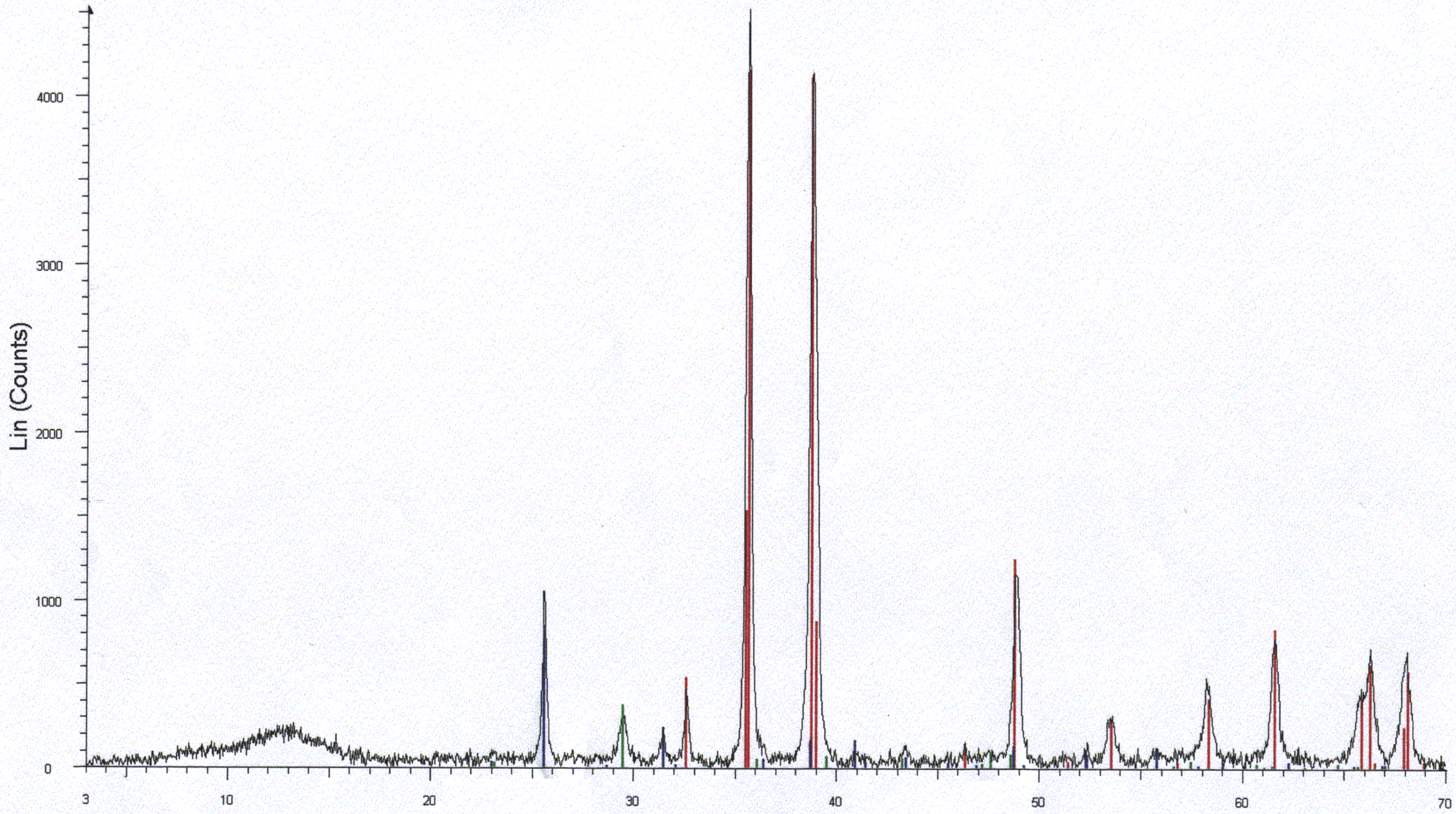

3 - File: RICCO01 .raw - Type: 2Th/Th locked - Start: 3.000 ° - End: 70.040 ° - Step: 0.040 ° - Step time: 1.5 s - Temp.: 25 °C (Room) - Time Started: 0 s - 2-Theta: 3.000 ° - Theta: 1.500 ° - Chi: 0.00 ° - P
48-1548 (*) - Tenorite, syn - CuO - Y: 92.12 % - d x by: 1. - WL: 1.5406 - Monoclinic -
37-1496 (*) - Anhydrite, syn - CaSO4 - Y: 18.75 % - d x by: 1. - WL: 1.5406 - Orthorhombic -
47-1743 (C) - Calcite - CaCO3 - Y: 8.33 % - d x by: 1. - WL: 1.5406 - Rhombohedral -

XRF REPORT:

University of Pretoria
Pretoria 0002 Republic of South Africa Tel (012) 4209111
Fax (012) 43-6867

Faculty of Science
XRD & XRF Laboratory
Department of Earth Sciences
Tel.: (012) 420 2137
Fax.: (012) 362 5219
e-mail: mloub@scientia.up.ac.za

CLIENT: Isabel Ricco

DATE: 20 April 2001

SAMPLES: CuO samples

ANALYSIS:

The sample was mounted on a thin film and analysed using the ARL9400XP+ spectrometer with the wide confidence limit program. Due to the very small sample used these values are not exact but indicative of the impurities present.

%	SAMPLE1	SAMPLE2	SAMPLE3
SiO_2	1.52	n/d	n/d
TiO_2	n/d	n/d	n/d
Al_2O_3	1.92	n/d	n/d
Fe_2O_3	0.49	0.74	n/d
MnO	0.25	0.32	0.53
MgO	1.41	0.36	0.63
CaO	18.5	0.61	0.69
Na_2O	n/d	n/d	n/d
K_2O	n/d	n/d	n/d
P_2O_5	0.21	0.11	0.11
SO_3	19.1	n/d	n/d
Cr_2O_3	940 ppm	n/d	n/d
NiO	0.54	0.29	0.20
CuO	55.5	97.3	97.8
ZnO	0.41	0.27	n/d

If you have any further queries, kindly contact the laboratory.

Analyst:

M.Loubser

APPENDIX E

BURN RATE MEASUREMENTS FOR INITIAL TRIALS

All burn speeds are in mm/s. All runs under 1 were run in Nov 01 and all runs under 2 were run Feb. 02. The samples of PbCrO4 were lost

A) CuO and Si

Method of intitiation	Mass oxidant	Mass Si	Fuel:Total mass ratio	AEL tests	1			2		
					mm	Comment	Burn speed	mm	Comment	Burn Speed
Shock Tube	25.309	4.691	15.63667	Did not ignite	4	Mixture Failure		10	Shock Tube Failure	
Starter					5	Mixture Failure, heat due to starter element		10	Mixture Failure, heat due to starter element	

B) MnO2 and Si

Method of intitiation	Mass oxidant	Mass Si	Fuel:total mass ratio	AEL tests	1			2		
					mm	Comment	Burn speed	mm	Comment	Burn Speed
Shock Tube	17.218	2.789	13.94012	Burnt with sealer,	5	Mixture Failure		10	Shock Tube Failure	
Starter				Burnt with sealer and starter	5	Mixture Failure, heat due to starter element		10	Mixture Failure, heat due to starter element	

C) CuO.MnO2 (Prepared by Serei) and Si

Method of intitiation	Mass oxidant	Mass Si	Fuel:total mass ratio	AEL tests	1			2		
					mm	Comment	Burn speed	mm	Comment	Burn Speed
Shock Tube				Did not ignite	5	Mixture Failure		10	Shock Tube Failure	
Starter					5	Mixture Failure, heat due to starter element		10	Mixture Failure, heat due to starter element	

D) Cu(SbO2)2 (Prepared by Serei) and Si

Method of intitiation	Mass oxidant	Mass Si	Fuel:total mass ratio	AEL tests	1			2		
					mm	Comment	Burn speed	mm	Comment	Burn Speed
Shock Tube				Burnt with sealer,	5	Mixture Failure		10	Shock Tube Failure	
Starter				Burnt with sealer and starte	5	Burnt	9	5	Burnt	25

E) CuO.Fe2O3 (Prepared by Serei) and Si

Method of intitiation	Mass oxidant	Mass Si	Fuel:total mass ratio	AEL tests	1 mm	1 Comment	1 Burn speed	2 mm	2 Comment	2 Burn Speed
Shock Tube				Did not ignite	4	Mixture Failure		10	Mixture Failure	
Starter					4	Mixture Failure, heat due to starter element		10	Mixture Failure, heat due to starter element	

F) Fe2O3 and Si

Method of intitiation	Mass oxidant	Mass Si	Fuel:total mass ratio	AEL tests	1 mm	1 Comment	1 Burn speed	2 mm	2 Comment	2 Burn Speed
Shock Tube	9.161	0.808	8.105126	Did not ignite	5	Mixture Failure		5	Mixture Failure	
Starter					5	Mixture Failure, heat due to starter element		5	Mixture Failure, heat due to starter element	

G) Fe3O4 and Si

Method of intitiation	Mass oxidant	Mass Si	Fuel:total mass ratio	AEL tests	1 mm	1 Comment	1 Burn speed	2 mm	2 Comment	2 Burn Speed
Shock Tube	18.855	1.14	5.701425	Did not ignite	5	Mixture Failure		5	Mixture Failure	
Starter					5	Mixture Failure, heat due to E element		5	Mixture Failure, heat due to E element	

H) Fused V2O5 and Si

Method of intitiation	Mass oxidant	Mass Si	Fuel:total mass ratio	AEL tests	1 mm	1 Comment	1 Burn speed	2 mm	2 Comment	2 Burn Speed
Shock Tube	18.571	1.435	7.172848	Did not ignite	5	Mixture Failure		5	Mixture Failure	
Starter					5	Mixture Failure, heat due to starter element		5	Mixture Failure, heat due to starter element	

I) Deamm V2O5 and Si

Method of intitiation	Mass oxidant	Mass Si	Fuel:total mass ratio	AEL tests	1			2		
					mm	Comment	Burn speed	mm	Comment	Burn Speed
Shock Tube	18.561	1.438	7.19036	Did not ignite	5	Mixture Failure		5	Mixture Failure	
Starter					4	Mixture Failure, heat due to starter element		5	Mixture Failure, heat due to starter element	

J) Sb2O3 and Si

Method of intitiation	Mass oxidant	Mass Si	Fuel:total mass ratio	AEL tests	1			2		
					mm	Comment	Burn speed	mm	Comment	Burn Speed
Shock Tube	17.479	2.539	12.68358	Burnt with starter and sealer	10	Shock Tube Failure		5	Mixture Failure	
Starter					4.5	Burnt	3	5	Burnt	2

APPENDIX F

VARYING STOICHIOMETRY

EXPERIMENTAL DATA FOR TUMBLE MIXED COMPOSITIONS

APPENDIX G

VARYING STOICHIOMETRY

EXPERIMENTAL DATA FOR TUMBLE AND BRUSH MIXED COMPOSITIONS

APPENDIX H

VARYING STOICHIOMETRY AND SILICON PARTICLE SIZE EXPERIMENTAL DATA

APPENDIX I

VARYING OXIDANT PARTICLE SIZE EXPERIMENTAL DATA

APPENDIX J

ALUMINIUM ADDITION

EXPERIMENTAL DATA

APPENDIX K

FUMED SILICA ADDITION EXPERIMENTAL DATA

APPENDIX L

THE USE OF DISPERSIONS AS A PROCESSING ROUTE

PROPOSAL

L1 DISPERSIONS AND DISPERSANTS

Dispersions occur when two or more phases are insoluble or slightly soluble and are dispersed in one another. The continuous or external phase is termed the dispersion medium while the substance distributed in it is termed the internal or dispersed phase (Heusch, 1993:577).

The energy required to produce a dispersion increases with decreasing particle size because their surface area increase and the energy (W) is directly proportional to the surface area (S), i.e.:

$$dW_1 = \gamma_1 dS$$

From the equation, it can be seen that as the surface tension (γ) of the fluid increases, so does the energy required to produce the dispersion. Dispersants lower the interfacial tension between the phases (Heusch, 1993:577). They thus help maintain fine solid particles in a state of suspension and inhibit the particles from agglomeration or settling in the fluid medium.

L1.2 The Dispersion Process

The preparation of a dispersion entails three stages, i.e.

- Wetting the powder into the liquid medium
- Deagglomerating the wetted clumps and
- Preventing reagglomeration or flocculation (Nelson, 1996:1093).

L1.2.1 Wetting the Powders

In order to overcome surface defects such as:

- Lattice defects
- Non-stoichiometry
- Impurity ions
- Dislocations and

- Surface roughness

a solid will tend to adsorb polar molecules such as water i.e. oxygen or hydroxyl radicals cover the exposed surfaces (Focke, 2000a). Despite this, the wetting of powders remains a problem. The wetting process consists of three mechanical steps: adhesion, immersion and spreading. Nelson (1996:1094-1096) has described the fundamentals for the wetting of single particles and clumps. A more detailed discussion of the wetting phenomenon with an approach based on the theory of surface forces has been made by Churaev (1995).

The most common wetting agents are anionic surfactants chosen from the families of alkali, sulphonates, sulphates, ligno sulphates, carboxylates and phosphates. The optimum chain length is between 12 and 18. A wetting agent with a low molar mass has a high diffusion coefficient and thus has a faster rate of wetting. The selection of the wetting agent is important, as the agent may interfere with the drying of the powders in the downstream processing (i.e. in the case of the delay elements the loading of the lead tubes may be affected).

Gas that is drawn beneath the surface of the liquid as a result of a vortex or plunging jet, due to the high shear which is used, may be dispersed into small bubbles which may be stabilised by the wetting agent to form a stable foam. The amount of wetting agent that should also be limited for this reason (Nelson, 1996:1096). Typically only 0.01 to 0.2% (mass basis) of the wetting agent is added to the dispersion (Focke, 2000c)

L1.2.2 Deagglomerating the Wetted Clumps

The particles in a dry powder are held together by the polarisability attraction of adjoining particles, the surface tension at wetted contacts or moderately strong sintering or precipitation bonds. These bonds are formed at the contact points because of the exposure to humidity and temperature cycles during storage before use. Breaking these bonds to fully disperse the submerged and wetted clumps requires high shear stress or mechanical impact. This will result in the formation of a small amount of new surface area that may have a higher adsorptivity and reactivity than the rest of the clump. Methods for the deagglomeration of pigments, which a few of the

constituents in the pyrtechnic formulations are, have been described in ISO 8780 – parts 1-6 (Nelson, 1996:1097-1098).

L1.2.3 Preventing Reagglomeration

Factors Affecting Reagglomeration

The factors which affect dispersion stability have been discussed in detail by Nelson (1996:1100-1104).

- *Polarisability Attraction*

All matter is composed of electric charges which move in response to an external field which can be created by the distribution and motion of charges in nearby matter. The Hamaker constant for interaction energy is a measure of this polarisability attraction between the particles. The determination of the Hamaker constant has been described by numerous authors (Nelson, 1996:1100; Drummond & Chan, 1997; Nguyen, 2000; Bergström, 1997; Reiter *et al*, 1999). Higher constants indicate greater attraction (Hann, 1996:298). The following Hamaker constants have been reported in literature (Table L-1).

Table L-1: Hamaker Constants (Lafuma, 2000)

Particle	**Hamaker Constant (10^{-20} J)**
Silicon	25.5
Water	4.35
Oxides	10.6 – 15.5
Metals	16.2 - 45.5

Nelson (1996:1100) has used the example of two identical spheres with diameter d separated in a liquid by a distance s, to describe the attractive energy, u, due to the attraction, i.e. when s=0 then u becomes infinite. A strongly adsorbed layer of liquid or other solute limits s to s_{min}, which may be set equal to twice the molecular diameter of the liquid, and u to the maximum value (Nelson, 1996:1100).

- *Thermal Jostling or Particle Motion*

If the thermal energy ($u_{thermal}$=kT as per convention) of the particles exceeds the maximum attractive energy u, then the thermal jostling is sufficient to disrupt the agglomerates and often keep the particles dispersed (Nelson, 1996:1100; Hann, 1996:296). Thus by increasing the temperature, agglomerates may be broken and particles may be dispersed. If, however, the particles collide with enough energy and are not well dispersed, they will coagulate or flocculate.

- *Sedimentation*

If the particles are more dense than the liquid medium, then they will move downwards and the bed of particles which is formed compresses toward the state of minimum-included liquid. The property of minimum included water is desirable for the processing of pyrotechnics, as the presence if water in the mixtures affects the burn rate, i.e. small amounts of water have been known to accelerate the burn rate of lead dioxide-silicon mixtures (McLain, 1980:43). If the product of the height of the container and the sedimentation force of the particles (due to gravity or centrifugation) is greater than the thermal energy, then the particles will settle in a dense bed at the bottom (or top if the particle density is greater than the density of the liquid) (Nelson, 1996:1100-1101).

- *Viscous Drag*

The viscosity of the liquid limits the velocity with which the particle can move through the liquid in response to an external force. The balance between the forces on the particle due to gravity and viscous drag determines the terminal sedimentation velocity (Nelson, 1996:1101).

- *Electrostatic Interactions*

Particles with like charges repel each other. The charges may be as a result of hydrolysis (which will be discussed later) of the surface groups or adsorption of ions from the solution. The Stern layer is defined as the layer of solution immediately adjacent to the surface that contains the counterions not part of the solid structure but which are bound so strongly to the surface that they do not exchange with the solution. The plane separating the Stern layer from the next is known as the Stern plane and has a smaller potential than at the surface. At the shear plane, the motion of

the fluid relative to the particle is equal to zero. For particles with no adsorbed surfactant or ions, this plane is at the particle surface. Adsorbed surfactant or ions that are strongly attracted to the particle, prevent liquid motion close to the particle, thus moving the shear plane away from the particle surface. The effective potential at the shear plane is known as the zeta potential that may be used to determine the electrostatic repulsion force. If the electrostatic repulsion exceeds the polarisability attraction at the distance of closest approach, determined by the surrounding fluid, then the particles may be prevented from coming into contact unless they are in a bed of sediment and are pressed together due to its weight (Nelson, 1996:1102-1103).

- *Polymer Chain Interactions*

If the particle is covered with links to polymer chains that are soluble in water, then the particles will be sterically hindered from coming together. If the chains extend a distance of δ_1 into the liquid, then according to Nelson (1996:1103), unlike electrostatic and polarisability interactions which act over large distances, steric repulsive interactions act only when $s<2\delta_1$.

Surface Modification

Reaction or adsorption at the solid surface alters the properties and lead to a surface charge or steric stabilisation.

- *Hydrolysis*

Inorganic particles have a surface charge in water that is a function of the particle's character and the pH. The surfaces of metal oxides, which are the primary constituent of the formulations, can be hydrolysed and take up H^+ or OH^- ions and become charged. Aqueous solutions may sustain potentials as high as 100mV. This potential is a function of the pH. The zeta potential is a measure of the electrostatic potential at the Stern layer that surrounds the particle. The zeta potential for the particle is positive if the solution pH is below the particle's isoelectric pH and negative if it is above the isoelectric pH. According to Nelson (1996:1105) a zeta potential greater than 30mV (positive or negative) is sufficient to keep the particles well dispersed. Lower values may be sufficient for particles with weak attractive forces (Hamaker

Constant close to that of the liquid), but not for particles with strong interactions (Nelson, 1996:1104-1105 & Hann, 1996:294-296).

It is possible to measure the surface charge of a particle using titration. The following points of zero charge or isoelectric pH values have been reported in literature:

- Fe_2O_3 (synthetic or freshly formed in water) – 8.6 (Lafuma, 2000b), 8.0 – 8.7 (Hann, 1996:295)
- Fe_2O_3 (dehydrated) – 5.2 (Hann, 1996:295)
- SiO_2 – 2.2 (Hann, 1996:295).
- Si – above 2, the zeta potential has been reported as being negative (Hackley *et al*, 1997)

This means that at a pH of 7 synthetic or freshly formed Fe_2O_3 will be attracted to Si, whereas dehydrated Fe_2O_3 will not be attracted to Si.

- *Differential Dissolution or Complexation*

In the case of ionic salts, one of the ions making up the lattice may be complexed or hydrated more readily than the other resulting in an imbalance in the particle charge. The surface charge of the particle will thus change with the solution composition as the degree of complexation is affected by additives that adsorb on the surface, complex with the ion or affect the ionic strength and hence the distance over which the particle potential is effective (Nelson, 1996:1105).

- *Chemical Grafting*

Polymer chains which are soluble in the liquid may be grafted onto the particle and provide steric stabilisation. Nelson (1996:1105) has stated that for typical interparticle potentials and a particle diameter of 10μm, steric stabilisation can be provided by a soluble polymer layer with a thickness of approximately 10nm, which can be provided by a polymer tail with a molar mass of 10kg/mol.

- *Surface Coating*

Semisteric stabilisation can be achieved by adding a dense surface coating that contains no occluded solvent, provided that the coating has a Hamaker constant, which is intermediate between the particle and the liquid (Nelson, 1996:1105-1106).

DLVO Theory

The overall stability of the particle dispersion depends on the sum of the attractive and repulsive forces as a function of the distance between the particles. The DLVO theory encompasses the attraction (as mentioned previously is a function of the Hamaker constant) and electrostatic repulsion between the particles (as mentioned previously is a function of the kinetic energy of the particle – thermal jostling; ionic strength, zeta potential and separation distance) but ignores steric stabilisation. The effect of the various variables as predicted by the DLVO theory has been summarised by Hann (1996:299) and can be found in Table L-2.

Table L-2: Effect of Increasing Various Variables on the Coagulation and Flocculation Resistance (Hann, 1996:299).

Variable	**Coagulation Resistance**	**Flocculation Resistance**
Particle size	Increase	Decrease
Surface potential	Increase	Increase
Electrolyte	Decrease	Decrease
Hamaker constant	Decrease	Decrease

Steric Stabilisation versus Electrostatic Stabilisation

Hann (1996:300) has summarised the practical differences between electrostatic and steric stabilisation. This summary may be found in Table.L-3

Table L-3: Practical Differences between Electrostatic and Steric Stabilisation

Steric Stabilisation	**Electrostatic Stabilisation**
Insensitive to electrolyte	Coagulation occurs with increased electrolyte
Effective in aqueous and nonaqueous media	More effective in aqueous media
Effective at high and low concentrations	More effective at low concentrations
Reversible flocculation common	Coagulation is often irreversible
Good freeze-thaw stability	Freezing induces irreversible coagulation

Stabilising Additives

Dispersants consist of molecules, which have one region that is soluble in the liquid and another which is slightly insoluble and attaches to the particles. The adsorbed dispersant prevents agglomeration either by steric stabilisation or by electrostatic stabilisation. The polarisability interactions attract the dispersant molecules from the solution onto the particle surface. If the adsorption sites are equivalent and do not interact with one another, then the fraction of the surface covered by the adsorbate, f, can be described by the following relationship:

$$f = \frac{K_{ads} C_{surf}}{1 + K_{ads} C_{surf}} \qquad \text{(A)}$$

Near monolayer coverage (f>0.95) can only be achieved if $K_{ads}C_{surf}$>19, which can be problematic for some dispersants since the solution concentration cannot be higher than the critical micelle concentration (CMC) (Nelson, 1996:1106-1107). Typical usage levels of high molecular weight dispersants is between 1-10% and for low molecular weight dispersants the level is between 0.5-2% for inorganic powders which the formulations are composed of (Mailwane, 2000).

Positive ions are attracted by the negatively charged surface of the solid particles and therefore will have a higher concentration near the surface than in the bulk. Meanwhile negative ions are repelled from the negative surface and will have a lower concentration near the surface. The ionic attraction or repulsion from the surface affects the non-ionic adsorption coefficient (Nelson, 1996:1107).

Short chain organics that are adsorbed may reduce the polarisability attraction between the particles, provided that its Hamaker constant is between that of the solid and the liquid medium and that the adsorption layer is thick enough. Adsorption does not follow the Langmuir adsorption profile described by equation A in aqueous systems for organic dispersants, as the tails adsorbed molecules at adjacent sites tend to attract each other strongly. Ionisable organic dispersants lose or gain protons in solution if it is within the right pH range. The ionic species may absorb on the

oppositely charged inorganic surface and provide semisteric stabilisation (Nelson, 1996:1107).

Nonionic polymeric units which have been hydrated such as polyethylene oxide are water-soluble and thus adsorb strongly to highly polar materials, whereas alkanes are adsorbed strongly on non-polar materials. The adsorption of these materials cannot be described using the Langmuir theory because the sites are not independent. Dispersants under this class include homopolymers, random block copolymers, diblock copolymers and comb polymers.

- Homopolymers consist of a series of identical segments. If their segments adsorb strongly on the particle, the polymer layer will have a compressed conformation (little occluded liquid) and provide semisteric stabilisation. Less strongly adsorbed homopolymers will coat the particles and be anchored by either loops or tails and provide steric stabilisation.
- Random copolymers consist of random length sequences of soluble segments interspersed with less soluble segments which adsorb onto the particle, while the more soluble segments form loops or tails extending into the liquid. The advantage of this type of polymeric unit over the homopolymer is that due to the separate anchor and soluble segments, there can be better control over the adsorbed layer depth and desorption. Thermal energy drives the motion of the loops and tails and provides a steric barrier. The thickness of this barrier is dependent on the solvent. In a good solvent it is roughly one-third of the fully extended length of the loop or tail.
- Diblock copolymers consist of one sequence of anchor segments and a second sequence of backbone segments. Like random copolymers, the lengths of these segments can be controlled to allow for control of the adsorbed layer depth and soluble segments.
- Comb polymers have a soluble backbone with a number of side chains that contain the anchor group (Nelson, 1996:1107-1108).

Drummond and Chan (1997) have studied the van der Waals interaction, surface free energies and contact angles for the following dispersive polymers and liquids:

- Polymers – Poly(dimethylsiloxane) (PDMS), poly(4-methyl-1-pentene) (TPX), polyethylene (PE), natural rubber and polystyrene (PS)

- Liquids – diiodomethane, 1-bromonaphthalene, 1-methylnaphthalene, bromobenzene, *tert*-butylnaphthalene, liquid paraffin and hexadecane (Drummond & Chan, 1997).

Adsorption of Microparticles

Nelson (1996:1109) has proposed that microparticles which diameters less than a tenth of the particles to be dispersed, can be attached to the larger particles by sintering prior to wet in. According to Nelson (1996:1109-1110), these particles will provide polarisability attraction if their Hamaker constant is midway between the liquid and larger particle or electrostatic attraction if the microparticles have a charge opposite to that of the larger particle. The attached microparticles will prevent the surfaces of the larger particles from coming close together, thus reducing the maximum attractive energy in the same way that encapsulation does (Nelson, 1996:1110). Solid state sintering occurs when a system of loose or compacted powders are subjected to heat treatment below the melting point of all its constituents (Kayser & Weise, 1993:118). Initially it was thought that this method could be used by sintering the Nanocat iron oxide with the silicon prior to dispersing the silicon with another reducing agent. This would allow for intimate contact between the silicon and one of the reducing agents (the Nanocat iron oxide). From the literature it appeared that the Hamaker constants could be in the right range. Despite these factors, this option cannot be used for the following reasons:

- It would entail the use of special crucibles (made from refractories such as ZrO_2 or borides of the transitions metals) which may be expensive
- The high energy cost of the sintering process
- The strong probability that during the sintering process, sufficient energy is added to ignite the mixtures and
- The practical implications of changing the formulation process that significantly in practice i.e. buying new equipment.

In summary, a dispersion can be stabilised if the maximum attractive energy is less than the thermal energy. It should be noted however that the polarisability attraction, electrostatic repulsion and steric repulsion increases with an increase in particle diameter, whereas thermal jostling is independent of the particle diameter.

L2 PROPOSED DISPERSION FORMULATION AIMS

The following aims would have to be achieved by the dispersion process:

- Wet the powders
- Break up particle clusters
- Ensure proper mixing
- Form dense, thin sediment layer of powders once they have settled using centrifugation
- Allow for easy drying
- Minimise the risk of fires when handling the dry powdered formulations downstream
- Allow for reproducible and desired burn speeds of the pyrotechnic formulations. The addition of the wetting agent and dispersant will also affect the amount of oxidising agent which is to be added. This is due to the fact that the carbon and hydrogen atoms in these compounds require oxygen during the burning process of which the oxidising agent is the only source as the reactions occur in sealed containers.
- The surfactant should also be compatible with water.

One of the problems that may be foreseen is that despite the powders being well dispersed in the liquid phase, upon settling, due to the density differences, there will be preferential settling of either the oxidising agent or the silicon. This could be overcome by either:

- Finding a surfactant or surfactant mixture that will not allow preferential settling or
- Shin *et al* (1998) have developed a deposition mechanism of oxide thin films on self-assembled organic monolayers. They developed the model because it has been proved that oxide thin films can be deposited on silicon wafers at low temperatures (<100°C) from an aqueous media using functionalised self-assembled which are ordered arrays of surfactant molecules (long chain hydrocarbons – chain lengths greater than 12CH_2 units) covalently attached to the substrate. The ordering of the surfactant molecules is as a result of the van der Waals interactions between adjacent hydrocarbon chains. It has been found that

both TiO_2 and ZrO_2 films precipitate on the sulphonate-functionalised self assembled monolayers and are adherent and uniform in thickness (Shin *et al*, 1998). This method could be modified to allow for the deposition of the desired reducing agent and not ZrO_2 or TiO_2 on the monolayer. This method would ideal as it allows for proper mixing and intimate contact between the particles – i.e. constant thermal conductivity and contact.

L3 The use of Dispersants and Surfactants for the Dispersion Formulation

L3.1 Finding the Best Wetting Agent

A "flotation" test can be used to determine the effectiveness of the wetting agent. The powder is distributed in the surface of a solution and the time taken by the particles to reach the bottom of the container is measured. This time is inversely proportional to the efficiency of the wetting agent (Mailwane, 2000).

L3.2 Choice of Surfactant – Influence of Surfactant Properties

The choice of surfactant and amount of surfactant used depends on a number of factors, i.e. the chemical nature of the hydrophile, the cmc of the surfactant

The following surfactant properties need to borne in mind when formulating the aqueous dispersions:

- Critical micelle concentration (CMC)- It will be necessary to operate below the CMC in order to avoid overdosing. Surfactants are also most effective at concentrations close to their CMC. The CMC is influenced by chemical structure, nature of counterions, temperature and pH.
- HLB-value – This classification is only used for only for the classification of nonionic surfactants. An increase in hydrophilicity results in an increase in the HLB. The typical HLB range for dispersions is 8-13. It is possible to get a measure of the HLB value from the solubility of the surfactant in water.

- Surfactant Type - Ionic surfactants work by electrostatic forces i.e. repulsion, while nonionic surfactants work by steric repulsion which is good for applications where the medium is polar i.e. water. If increase the electrolyte content of the medium, it will be possible to get close contact and flocculation. Polymeric surfactants are nonionic and contain segments that absorb strongly onto the particle and with a compressed conformation will lead to semisteric stabilisation.
- Water Hardness and Ionic Strength – Anionic surfactants will precipitate out as a result of the water hardness whilst nonionic surfactants will "salt" out of the aqueous solution as a result of the ionic strength (Bognolo, 2000)
- Solubility and Temperature – For ionic surfactants, if the temperature is increased above the Krafft temperature solubility will increase, whilst with nonionic surfactants if the temperature is increased above the cloud point, solubility will decrease.
- Other properties - Foam is an undesired property that can be overcome through the use of antifoaming agents (Broadbent, 2000). For stirred reactors and mixers foam can reduce the batch size. According to Farminer (1973), antifoams based on polydimethyl siloxane fluids have most of the desirable features necessary for controlling foam in any media, i.e. fast knockdown, long lasting action, high efficiency, low cost and ease of handling. These antifoams should, however, not be used where it is dissolved by components of the foaming system e.g. chlorinated hydorcarbon processing. The criteria for successful foam control are:
    - A lower surface tension than the foaming media
    - Insolubility in the foaming media and
    - Dispersibility in the foaming media (Farminer, 1973).

The polarity of the solids will have an effect the type of surfactant that is used. Generally for solids of low polarity long chain alcohols, POE and POE/POP may be used, whilst for highly polar solids alkylphenols, POE, POP/POE, unsaturated alcohols, block copolymers, di- and polyamides may be used (Bognolo, 2000).

L3.4 Method for Choosing the Right Surfactant

The following procedure has been proposed:

- Evaluate the surfactant solubility in the medium without the powders
- Measure the zeta potential of the particles in the medium – not use cationic dispersants if positive and anionic if negative
- Measure the viscosity of highly loaded suspension only powders and liquid (more than 40% solids) – eliminate one with higher viscosity and poor flow characteristics
- Observe sedimentation behaviour of 5 – 10% solids suspension – use only liquid and powders
- Eliminate the surfactant that gives large sediment volume and does not allow for constant and reproducible burn rates
- Check quality of complete dispersion using the British Standard (BS) 3466 (part 4) for metal oxides and ASTM standard B821-92 for metal powders or the methods contained in section 5 (Nelson, 1996:1109).

Due to their synergistic behaviour, it has been recommended that mixtures of surfactants be used. Unfortunately the mechanism of mixed surfactant adsorption is not understood (Penfold *et al*, 1998).

L4 Dispersant and Surfactant Literature for the Dispersion of the Individual Constituents of the Proposed Pyrotechnic Formulations

A vast amount of literature is available on types of dispersants. Comb graft copolymers such as methoxy polyethylene glycol with an acrylic copolymer backbone have been used with great success as a dispersant (Broadbent, 2000). Table L-4 contains examples of organic polymeric dispersants which Hann (1996:303) has summarised.

Table L-4:Examples of Dispersants (Hann, 1996:303).

Type	**Trademark Name**
Poly(meth)acrylates	Alcosperse, Aquatreat, Antiprex, Alcomer, Cyanamer, Belsperse, Goodrite, Acusol, Acumer, Tamol, Daxad.
Polymaleates	Sokolan, Belsperse, Belgard, Belasol, Norasol
Condensed phosphates	
Polysulphonates	Versa TL, Polyfon, Reax, Indulin, Vanisperse, Borresperse and Ultrazine
Sulphonated polycondensates	Lomar, Tamol
Tannins, lignins, glucosides, alginates	Marasperse

Polyacrylates are the most flexible because they are produced in a variety of molecular weights and degrees of anionic charge. Polymaleates are very similar to polyacrylates, but maleic acid is not as easily copolymerised with other functional monomers to allow tailoring for specific applications. Condensed phosphates are not used as much today, due to the role that the phosphates play in the eutrophication of water bodies (Hann, 1996:302).

The following recommendations and studies have already been made and conducted respectively for the dispersion and wetting of the individual powders:

L4.1 Silicon

- Penfold *et al* (1998) used specular neutron reflection to measure the adsorption of the mixed cationic/non-ionic surfactant mixture of $C_{16}TAB/C_{12}E_6$ at the hydrophilic Si/SiO_2/aqueous solution interface. They found that the non-ionic/cationic surfactant adsorbed layer at the Si/SiO_2 interface is a fragmented bilayer. The adsorbed layer can thus be described by three layers. The first layer, adjacent to the solid surface, contains the head groups. The next layer is the associated hydration layer containing the hydrocarbon chains interpenetrating (or

overlapping) from both sides of the interlayer and the third layer adjacent to the fluid phase containing the head groups and hydration. The bilayers were found to be essentially symmetrical, the two headgroup regions appeared identical and the alkyl chain region was less than the dimension of a fully extended chain. This was attributed in part to the fraction of alkyl chains that were in the head group region as a result of the constraints arising from the disparity in head group size between the two surfactants (Penfold *et al*, 1998).

- Hackley *et al* (1997) have compared the dispersion properties of silicon powder with and without the use of surfactants. They found that the untreated silicon powder was easily dispersed and the results obtained were consistent with a model of the particle-solution interface based on the SiO_2-H_2O systems. The suspensions exhibited negative surface potentials at pH values exceeding 2 and were a maximum at pH 9. Furthermore, silicon that had been aged in an electrolyte solution had a higher surface potential, which they attributed to the increase in the surface site density of the Si-OH groups that occurred as a result of slow surface hydrolysis reactions. A summary of their results with various dispersants has been summarised in Table L-5.

Table L-5: Dispersion of Silicon using various Dispersants (Hackley et al*, 1997)*

Dispersant	**Findings**
Daxad 34 – anionic surfactant, linear poly(methacrylic acid) (PMAA)[1]	Had little effect on particle potential – weak interaction with the Si surface. But the adsorption on the negatively charged silicon was functionally similar to the adsorption behaviour for poly(acrylic acid) on Si_3N_4 and PMAA-Na^+ on Al_2O_3 at ph values above their isoelectric pH
Betz 1190 – dimethylamine-epichlorohydrin linear copolymer[2]	Resulted in a shift in the isoelectric pH with increasing polymer concentration (Saturation between 0.1 – 0.5%). Also resulted in a positively charged particle whose electrokinetic behaviour was independent of pH or polymer concentration

Dispersant	Findings
Daxad CP2 - dimethylamine-epichlorohydrin linear copolymer[2]	Similar to results obtained with Betz 1190
Betz 1195 – cross linked form of Betz 1190 with a higher M_r[2]	Similar to results obtained with Betz 1190

[1] A weak acid that dissociates to form an anion. Acid-base properties dependent on the solution pH.

[2] The copolymers are salts of quaternary ammonium compounds and therefore carry a positive charge regardless of the pH.

L4-2 Antimony Trioxide

Mailwane (2000) found during laboratory tests that calsoline oil appeared to be a good wetting agent for antimony trioxide.

L4-3 Iron Oxide

Homopolymers have been found to be ineffective for imparting steric stabilisation as the polymer chain prefers to associate with the solvent molecules of with the surface of the particle and not both at the same time (van der Avort, 1992). van der Avort (1992) has recommended that for metallic iron oxide (red) dispersion surfactants such as Hypermer CG6 (soluble graft copolymer), A109 (modified soluble polyester), PS2 (dispersible polyester) and Atlas G4911 (soluble POE alkyl aryl phenol). These are all nonionic surfactants, which provide steric stabilisation. The recommended dosage for metallic oxides is 1-3% based on the mass of solids (van der Avort, 1992).

L5 Dispersion Evaluation

The degree of deagglomeration can be evaluated using the following methods:

- *Viscosity* – The viscosity of a suspension that contains clumps decreases as the degree of deagglomeration decreases. This is attributed to the fact that the clumps contain occluded liquid and the volume fraction of the clumps is larger than the

volume fraction of the individual particles and so there is less free liquid to facilitate the flow than if the clumps were deagglomerated. This method of evaluation has a few inherent disadvantages, i.e. it is not sensitive in the final stages of deagglomeration.

- *Particle Size Distribution* – The degree of deagglomeration can be monitored using either sieving (particles >20μm) or instrumental particle size analysis for smaller particles.
- *Tinting Strength* – When the particles are well dispersed, they block more light than when there are clumps. Samples have to be taken at various intervals and a fixed quantity of well dispersed contrasting colour pigment added. The samples can then be analysed using a sensitive colorimeter. This method of evaluation cannot be used if the pigment is agglomerated by the sample or the sample and pigment settle out.
- *Grind Gauge* – This method has been described by Nelson (1996:1110). It cannot be used as it involves scraping an excess amount of sample, which is a paste. This may ignite the more sensitive pyrotechnic mixtures. The results obtained using this method are also subject to considerable variations.

The stability to reagglomeration may be evaluated using the following procedures:

- *Microscopy* – The optical microscope may be used for the evaluation of dilute suspensions (<1% solids) of particles 1-10μm. If the dispersion stable, thermal jostling can be seen and the particles will avoid coming close to one another or separate soon after collision.
- *Sediment Volume* – A stable dispersion will result in a thin sediment bed with maximum solids packing and minimum occluded liquid as the particles will move freely past each other to avoid contact as long as possible. Centrifugation will have to be used to force the particles to settle within a reasonable time.
- *Other* Other methods that could be used include the response to electric and acoustic fields, spectroscopy and drift in tinting strength (Nelson, 1996:1110-1111).
- *Ultrasonic Characterisation* – Guidarelli *et al* (1998) used ultrasonic attenuation to analyse suspensions of alumina powder in water at high concentrations (40% vol.). The purpose of their study was to identify weak structural differences that

occur between suspensions with different degrees of deflocculation, obtained by varying the quantity of dispersant around the critical value. This is difficult to be determined using other methods. They found that weakly flocculated suspensions presented lower attenuation than well flocculated suspensions (Guidarelli *et al*, 1998).

Hackley *et al* (1997) have measured the electrokinetic sonic amplitude (ESA) for silicon powder suspensions using an electoacoustic analyser equipped with an autotitrater, overhead stirrer and pH, temperature and conductivity probes. The ESA signal is proportional to the zeta potential and provides a convenient method of determining the polarity and relative magnitude of the charge carried by the particles. The titration data also provide a measure of the particle potential as a function of the pH and can thus be used to determine the isoelectric point (Hackley *et al*, 1997).

The easiest variables to measure for the evaluation of the dispersion would be viscosity, particle size distribution and sediment volume.

L6 DISPERSION PROCESSING EQUIPMENT

Nelson (1996:1098-1099) has described typical design elements for the wet in of powders and wet deagglomeration, the selection of which depends on the application It appears that for the dispersion of the pyrotechnic formulations the equipment in Figure L-1 for the following reasons:

- The disk impeller provides a rapidly refreshed liquid surface by creating a deep vortex. This exposes a new surface area for the powder addition
- The up and downward teeth at the edge of the impeller cause impact, turbulence and cavitation
- The baffles force vertical circulation.
- The equipment promotes rapid wet in due to the low gas pressure, high centrifugal force and the distribution of the powder in a thin and deagglomerated layer on the liquid
- The provision for the flow of clear liquid down the sides of the equipment aids in the prevention of scale and encrustation. Scale forms above the level when

airborne dust sticks to a wall wetted either by vapour condensation of liquid being drawn up the wall by capillary action through previously deposited scale. Encrustation forms near the shoreline of the tank as a result of the wetting and recession due to hydraulic pulses during agitation and then drying near that level. These two properties are undesirable in the processing of pyrotechnic powders as they lead to contamination of the batches which are prepared, the encrustation allows for a dry exposed areas which are easily ignitable and lastly during the processing and subsequent cleaning of the equipment of hazardous powders such as red lead, operators will be exposed directly to the powders (Nelson, 1996:1097&1099).

- A limitation of such a system is the heat that is generated to the high shear. Care should be taken not to have a high solids loading as this will increase the viscosity and hence the shear.

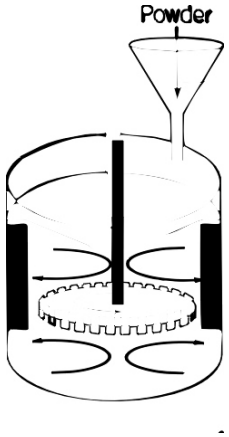

Figure L-1: Processing Equipment for Pyrotechnic Powder Wetting and Deagglomeration (Nelson, 1996:1098-1099).

Penfold *et al* (1996) have studied the effect of shear on the adsorption of a non-ionic surfactant at the silicon/solution interface using a specially constructed shear cell for neutron reflectivity measurements. They found that the hexaethylene glycol monohexadecyl ether ($C_{16}E_6$) there was evidence of shear induced structures in the vicinity of the cell wall. Furthermore at low surfactant concentrations ordered layering of the surfactant separated by solvent-rich regions and extending into the bulk solution was observed, in addition to the adsorbed layer on the solid surface. The

application of Poiseuille shear flow induced a more ordered and well defined structure at the interface (Penfold *et al*, 1996).

APPENDIX M

DISPERSION OF TYPE 4 SI AND CUO

EXPERIMENTAL DATA